Chapter 15

Multiresolution Tomography of Ionospheric Electron Density

T. Panicciari, N.D. Smith, F. Da Dalt, C.N. Mitchell and G.S. Bust

Additional information is available at the end of the chapter

http://dx.doi.org/10.5772/58772

1. Introduction

The ionosphere is an ionized medium which affects the electromagnetic signal that travels through it. The state of the ionosphere is studied in terms of Total Electron Content (TEC). This is a measurable observation, that in our case, is obtained from an estimation of the delay of the signal transmitted from a satellite and received at a ground station [1,2]. Computerized Ionospheric Tomography (CIT) uses a collection of observations to estimate the state of the ionosphere. CIT is also denoted as an inverse problem.

A 2D imaging of the ionosphere based on medical imaging was formerly proposed by Austen et al. [3], where a satellite in polar-orbit was used to collect TEC observations from a chain of ground receivers. There are substantial differences between medical and ionospheric scenarios mainly due to the geometry of the problem. CIT has, in fact, limitations such as limited angle observations and uneven/sparse distribution of the ground stations [4, 5] that make the solution unstable and difficult to solve. However, the capability of the method was demonstrated by Mitchell et al. [6] where, along a quasi-2D plane, features in the electron density were revealed at mid and auroral latitudes. Other research groups have successfully developed their CIT algorithms which are reviewed in Bust and Mitchell [7].

Geometric limitations cause the reconstruction to be underdetermined, especially where data are not available (e.g. in the oceans gaps). In general, a proper regularization is needed to compensate for where no data is available in order to reduce artefacts and noise within the results. Most of the algorithms are based on Tikhonov regularization [8], but another recent approach, new for CIT, is based on sparse regularization [9]. An implementation of this is given by the Fast Iterative Shrinkage-Thresholding Algorithm (FISTA) [10, 11]. A description of the

sparse regularization for CIT will be described in a forthcoming paper. This technique is used to overcome the limitation in the horizontal representation of ionospheric structures due to the uneven and sparse distribution of the ground receivers using simulated data.

An experiment is demonstrated here, using real data, where the advantages of sparse regularization using wavelets are illustrated over a standard implementation using spherical harmonics. TRANSIT data from the data set in [12] is also used. This data set consists of three Coherent Ionospheric Doppler Receivers (CIDRs), developed at Applied Research Laboratories at the University of Texas (Austin) and capable of observing the signal from TRANSIT system. Some results are presented comparing the Incoherent Scatter Radar (ISR) located in Sondrestrom (Greenland) and the CHAMP satellite. CHAMP data are from the Digital Ion Drift-Meter (DIDM) instrument provided by Air Force Research Laboratory (AFRL, Hanscom).

Section II illustrates the problem and solutions using two different regularization techniques. The data used for the reconstruction and comparison are described in Section III. Results and conclusions are presented in Section IV and Section V.

2. Method

TEC observations z are collected from ground receivers. They are in the form of Slant Total Electron Content (STEC) and are described according to the following equation (forward problem)

$$\boldsymbol{z=An+c} \tag{1}$$

where$z$ is the vector containing the uncalibrated observations of STEC, **A** is the projection matrix of geometry that maps the electron density n into the observations z. The vector n is described through the matrix of basis functions **K** and basis function coefficients x

$$\boldsymbol{n=Kx} \tag{2}$$

The matrix **K** defines the basis functions that we need in order to define the vertical and horizontal variation of the electron content. For the purpose of this paper we will focus on the horizontal basis functions, while vertical basis functions are described by Empirical Orthonormal Functions (EOFs) [13, 14].
The c term of (1) takes into account the fact that z is uncalibrated. Therefore the observations are affected by some biases c. They are solved together with z, to find the solution of the inverse problem of (1).

We solved the inverse problem of (1) by using two different regularizations:

- Tikhonov regularization. In this case, all the coefficients are used to estimate the state of the ionosphere. The method seeks to minimize the energy of the coefficients in some sense. Spherical harmonic basis functions are used in this case.
- Sparse regularization. The solution is solved with the Fast Iterative Soft-Thresholding Algorithm (FISTA) [10, 11]. It is particularly tailored for wavelet basis functions due to their ability to compact the information. The method seeks to minimize the number of basis functions needed to represent the structures in the ionosphere fittingly.

Both regularizations can guarantee a unique solution under certain conditions [15].

3. Data

Two different case studies are proposed using as comparison the Incoherent Scatter Radar (ISR) located in Sondrestrom (Greenland) and CHAMP satellite. Those case studies are representative of perturbed (kp=6) and quiet ionosphere (kp=2).

The first case study (kp=6) is based on a chain of TRANSIT receivers across Greenland together with GPS receivers. They recorded data during the day of the 30th September 2000, where data were collected within a time window of 9 minutes, with a sample rate of 30 seconds.

Fig. 1 shows the receivers, TRANSIT (red) and GPS (blue), used for the reconstruction together with the ray coverage. The TRANSIT satellite (ID18362) pass (purple) is also shown. The location of the ISR is illustrated with a black circle, and the scan path is indicated with a black solid line. For the present experiment only two of three TRANSIT receivers were available.

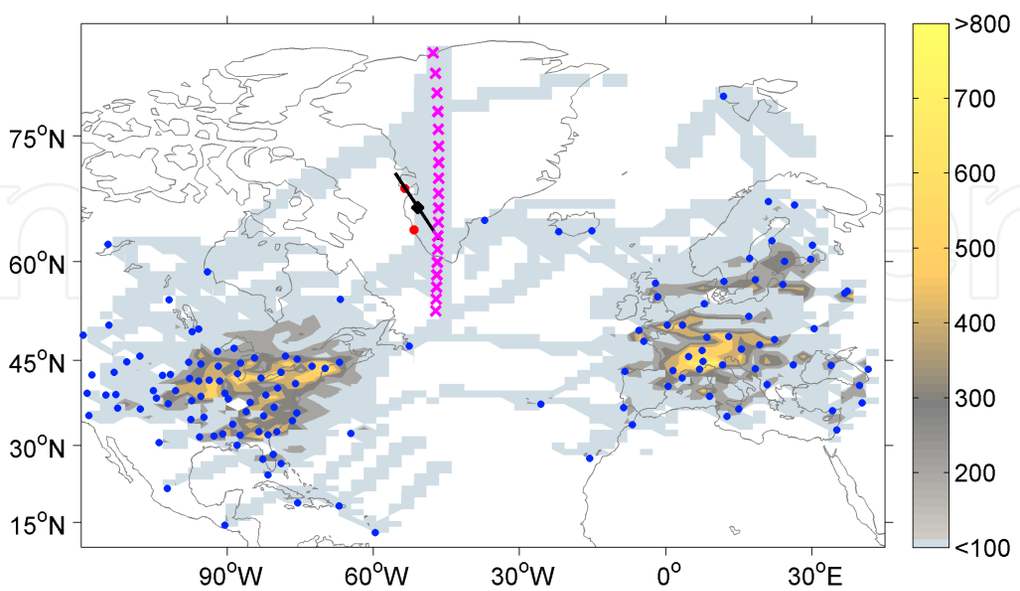

Figure 1. Number of rays and GPS ground stations (blue), TRANSIT ground stations (red), TRANSIT satellite pass (purple) and radar scan path (black).

The second case study (kp=2) used GPS receivers only for the day of 7th October 2002. Data sample rate was 30 seconds within a time window of 9 minutes. Fig. 2 shows the data coverage, GPS receivers (blue) and the southward CHAMP satellite pass (cyan).

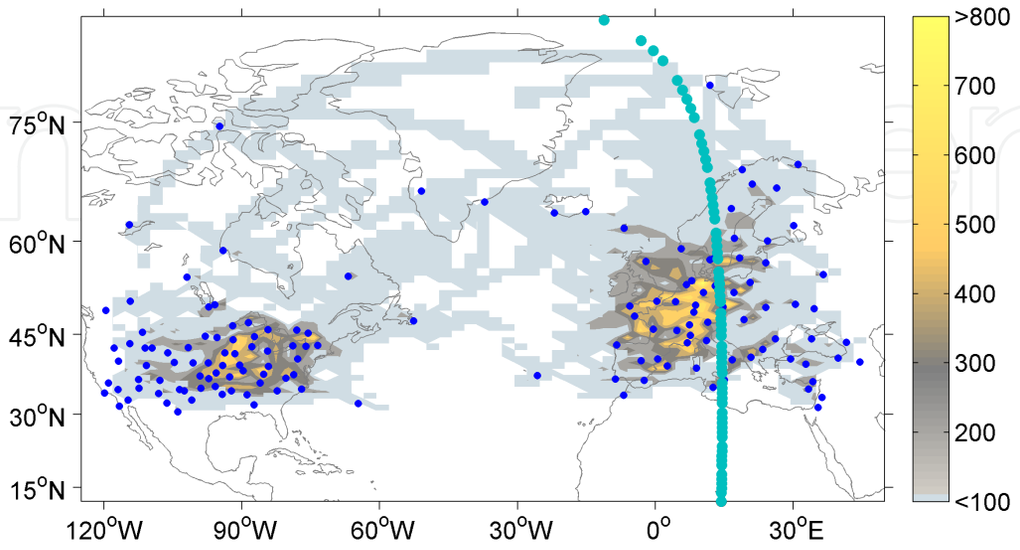

Figure 2. Number of rays and GPS ground stations (blue) and CHAMP satellite pass (cyan).

4. Results

A grid of dimension 64x64x22 voxels was selected in longitude, latitude and altitude. It corresponds to a maximum resolution of about 1x2 degrees in latitude and longitude and 50km in altitude.

EOFs from Chapman profiles [16] were used to constrain the vertical profile to be physically meaningful. In contrast, Discrete Meyer (DM) wavelets and Spherical Harmonic (SH) basis functions were used to describe the horizontal variation of ionospheric structures. We compared the results obtained with discrete Meyer (DH) and Spherical Harmonic (SH) basis functions at two different resolutions (by selecting subsets of horizontal basis functions). An ISR scan was also used as validation.

Fig. 3 shows the reconstruction obtained with SH (left) and DM (right) for two different resolutions. Values are in 1016 electrons/m2.

The low resolution reconstruction is shown in Fig. 3a and 3b for SH and DM, respectively. They both show a reasonable reconstruction with structures that appear smooth and with little detail but DM has some edge effects.

Fig. 3c and 3d show the reconstruction for SH and DM at higher resolution. The number of coefficients is significantly increased and SH needs a stronger regularization. The stronger regularization damps many coefficients down and the reconstruction loses its smoothness

http://dx.doi.org/10.5772/58772

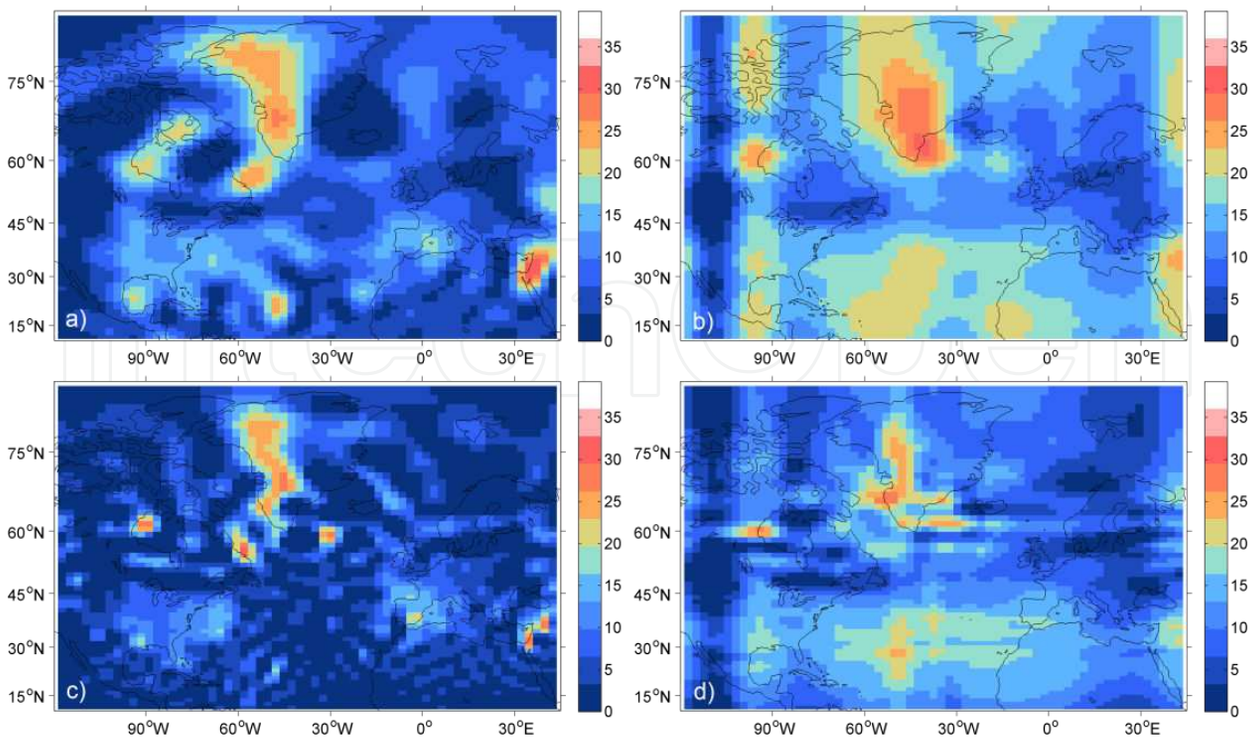

Figure 3. Low resolution reconstruction for: a) spherical harmonics; b) discrete Meyer; and high resolution reconstruction for: c) spherical harmonics; d) discrete Meyer. TEC values are in 10^{16} electrons/m^2.

(Fig. 3c) in comparison to the low resolution one (Fig. 3a). A ring oscillation phenomenon is also present due to the high number of basis functions to be estimated. This does not happen for DM. There are some lengthened structures (Fig. 3d) when using DM (between Greenland and Norway), which are mainly due to the particular data coverage (Fig. 1). Furthermore, DM reconstructs a structure located at 62°N 47°W (South of Greenland, Fig 3d), which is not present when using SH. In general, better performances can be obtained with a higher number of ground stations. The correctness of the results cannot be easily verified using real data due to the limited number of instruments that can be used for validation. The reliability of the methods described here will be illustrated in a forthcoming paper based on simulated data.

The sparse regularization aims to reconstruct the state of the ionosphere with the minimum number of basis functions. This makes the inversion stable, maintaining most of the information that was available at low resolution but better defining the edges of the reconstruction. This can be shown by comparing the reconstruction with the ISR scan that was available during the same time interval.

Fig. 4 shows a southward longitudinal ISR scan starting at 03:21:20UT on 30th September 2000. The scan has a duration of less than 4 minutes and values are shown in 1011 particles/m3. An enhancement can be seen towards the North while a depletion is evident in the South. In particular, a trough is present at the latitude of 64 degree.

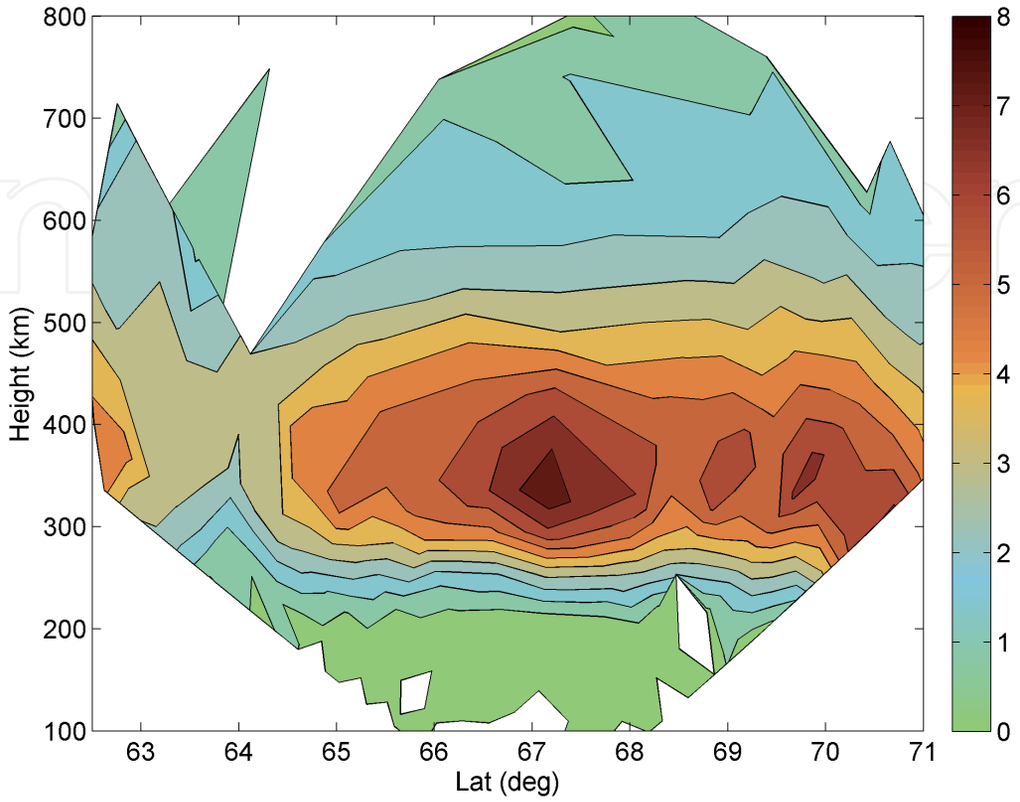

Figure 4. Southward longitudinal Incoherent Scatter (IS) radar scan starting at 03:21:20UT on 30th September 2000. Values of electron density are in 10^{11} particles/m^3.

Fig. 5a-5d show the electron density (10^{11} particles/m^3) of the reconstruction along the radar scan path for SH (left) and DM (right), and for low (top) and high resolution (bottom). The radar scan plane is aligned with the geomagnetic field lines and is tilted by about 27 degrees in the anticlockwise direction with respect to the reconstruction plane. The latter is instead aligned to the geographic coordinate system.

At low resolution SH produces a smooth profile (Fig. 5a), as DM similarly does (Fig. 5b). At higher resolution the depletion starts to be better defined and visible for SH (Fig. 5c). Both SH (Fig. 5c) and DM (Fig. 5d) show the same trough as well as a southward enhancement as indicated in the radar (Fig. 4); although the trough edges are more well-defined for DM (Fig. 5d). This is in agreement with the structure reconstructed in Fig. 3d using DM at 62°N 47°W.

Fig. 6a-b show a horizontal electron density profile from CHAMP (red) and from reconstruction (blue) during the day of the 7th October 2002. The CIT profile was extracted at the CHAMP altitude. A pale yellow background identifies latitudes where there is data coverage and it is over-imposed on a grey background that defines the CHAMP samples that were not in the time window used for the reconstruction. A dark grey is generated when the two backgrounds are overlapping.

http://dx.doi.org/10.5772/58772

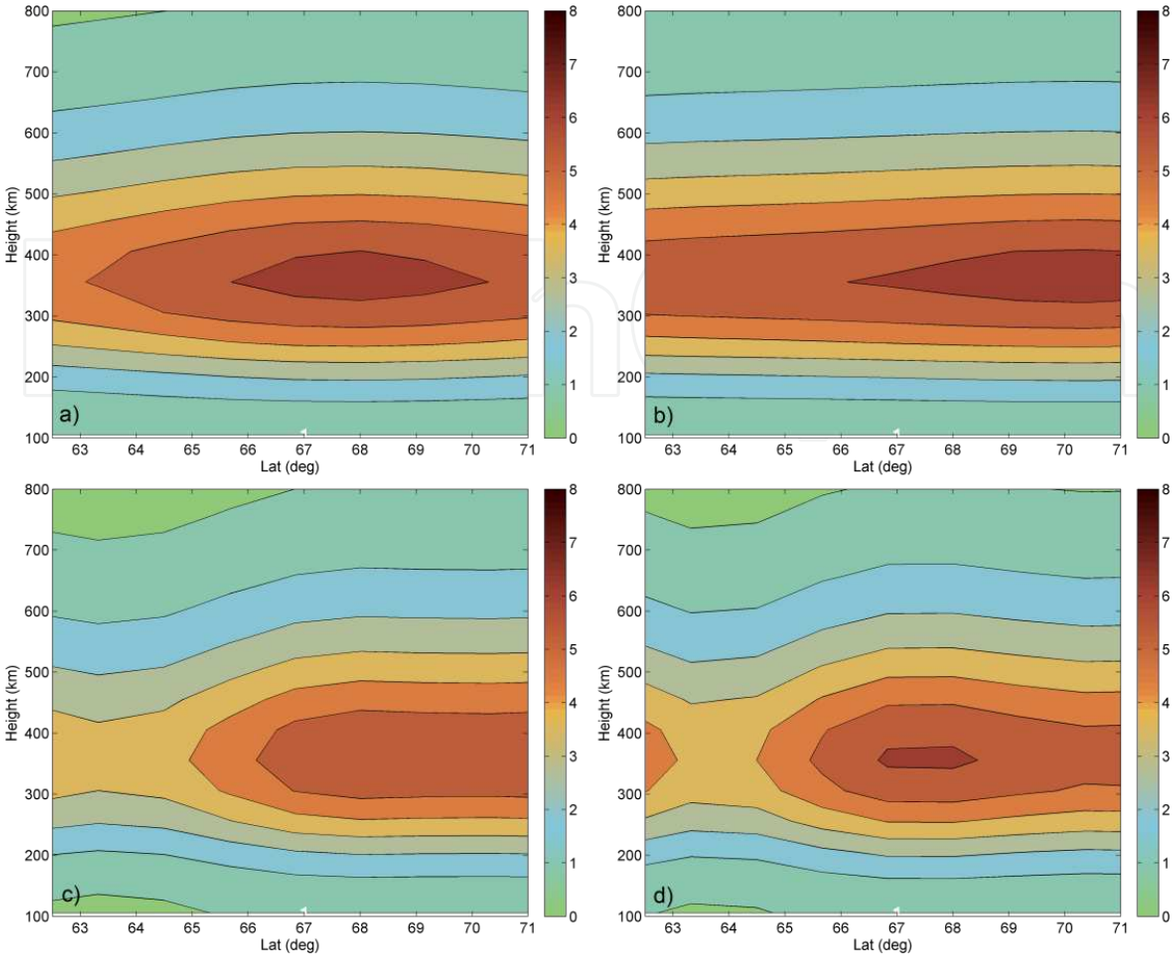

Figure 5. Cross sections from low resolution tomographic reconstructions for: a) spherical harmonics; b) discrete Meyer; and from high resolution tomographic reconstructions for: c) spherical harmonics; d) discrete Meyer. Values of electron density are in 10^{11} particles/m^3.

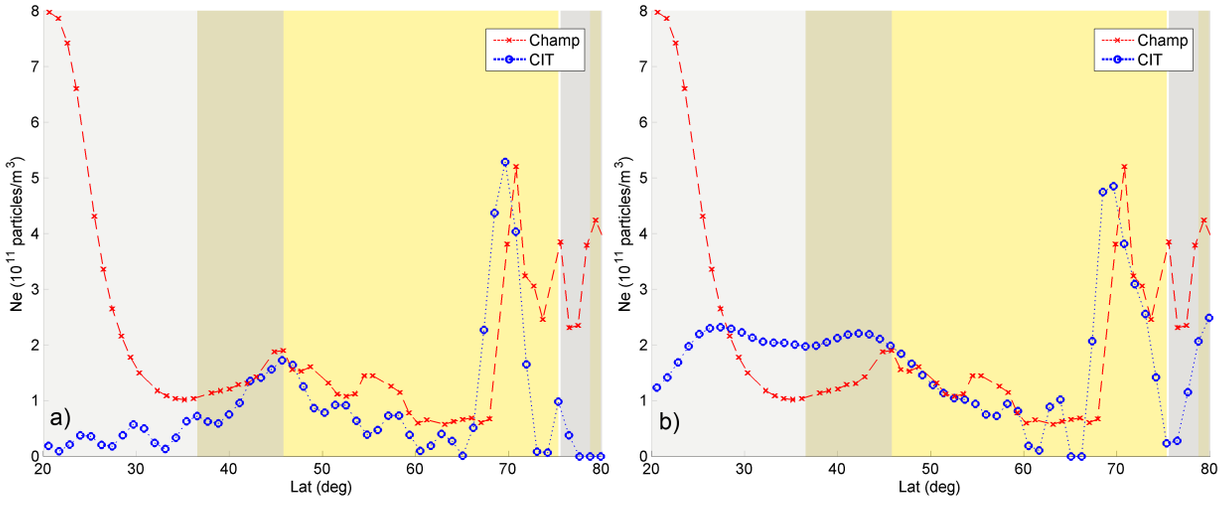

Figure 6. comparison of electron density from CHAMP (red) and CIT (blue) at high resolution using: a)spherical harmonics; b) discrete Meyer.

SH and DM reconstruct well the enhancement at about 70 degrees. It is noticeable the ring oscillation phenomenon for SH (Fig. 6a) while, for DM (Fig. 6b) that phenomenon is not present. DM seems also to estimate better the slope around 50 degrees. It is remarkable the different behaviour where data are not available. SH (Fig. 6a) decreases rapidly towards zero while DM reproduces a smooth enhancement before decreasing to zero. This is mainly due to the contribution of a large scale basis function that is used to represent the smooth part of the ionosphere. In that region the number of rays is small and not enough for resolving smaller features with smaller wavelets. SH (Fig. 6a) shows also the effect of a stronger regularization. The basis function coefficients are damped down and this causes an underestimation of the electron density.

5. Conclusions

Sparse regularization allows minimizing the number of basis functions that are needed for the reconstruction. Therefore, the algorithm estimates only the coefficients of a smaller subset of the entire set of basis functions; which in an underdetermined problem like in the Computerized Ionospheric Tomography (CIT) becomes of particular attractiveness. The reconstructions illustrated demonstrate sparse regularization as a valid alternative to Tikhonov regularization. Furthermore, sparse regularization seemed to preserve the information when the total number of coefficients to estimate increases. The results also show that the structure reconstructed at 62°N 47°W (South of Greenland) with sparse regularization is in good agreement with the radar scan. The same structure is not present with SH. This confirms wavelets and sparse regularization as a promising approach to detect different-scale structures of the ionosphere.

Better wavelet constructions may lead to further improvements in the reconstruction. In addition, the previous knowledge of the scales of structures that we could expect at different locations might likely help in the case of non-uniform or a small number of observations, to produce a smoother ionospheric reconstruction.

Acknowledgements

The authors acknowledge David Cooke (AF Research Lab) for CHAMP data, UNAVCO and IGS for GPS data. TRANSIT data were originally collected as part of a NSF project (ATM# 9813864) and ISR observations were supported by the NSF Cooperative Agreement AGS-0836152.

This research activity was supported by a Marie Curie initial training network (TRANSMIT) within the 7th European Community Framework Programme under Marie Curie Actions.

Author details

T. Panicciari[1], N.D. Smith[1], F. Da Dalt[1], C.N. Mitchell[1] and G.S. Bust[2]

1 Dept. of Electronic and Electrical Engineering, University of Bath, UK

2 Applied Physics Laboratory, Johns Hopkins University, USA

References

[1] Davies K.. *Ionospheric radio*. London: Peter Peregrinus. 1996. 600 p. doi: 10.1049/PBEW031E

[2] Mannucci A.J., Iijima B.A., Lindqwister U.J., Pi X., Sparks L., and Wilson B.D.. GPS and Ionosphere, in:W. Ross Stone (eds.). *Review of Radio Science 1996–1999*. Oxford: Wiley-IEEE Press. 1999. 625-665.

[3] Austen, J. R., Franke, S. J., Liu, C. H., Yeh, K. C. Application of Computerized Tomography Techniques to Ionospheric Research, in:*Proceedings of the Beacon Satellite Symposium 1986*. Finland. University of Oulu. 25-35.

[4] Yeh, K.C., Raymund, T.D.. Limitations of ionospheric imaging by tomography. *Radio Science*, 1991. 26(6): pp. 1361-1380. doi: 10.1029/91RS01873

[5] Na, H., Lee, H.. Analysis of fundamental resolution limit of ionospheric tomography, in:*Acoustics, Speech, and Signal Processing*. 23-26 Mar. San Francisco, CA. IEEE. 1992. 97-100. doi: 10.1109/ICASSP.1992.226267

[6] Mitchell, C.N., Jones, D.G., Kersley, L., Pryse, S. E., Walker, I.K.. Imaging of field-aligned structures in the auroral ionosphere. *Annales geophysicae*, 1995. 13: pp. 1311-1319. doi: 0992-7689

[7] Bust, G. S., Mitchell, C. N.. History, current state, and future directions of ionospheric imaging. *Reviews of Geophysics*, 2008. 46(1)doi: 10.1029/2006RG000212

[8] Tikhonov, A. N., Arsenin, V. Y.. *Solutions of ill-posed problems*. Winston. 1977. 258 p. doi: 0470991240

[9] Donoho, D.L.. For most large underdetermined systems of linear equations the minimal ℓ1-norm solution is also the sparsest solution. *Communications on pure and applied mathematics*, 2006. 59(6): pp. 797-826. doi: 10.1002/cpa.20132

[10] Beck, A., Teboulle, M.. A fast iterative shrinkage-thresholding algorithm for linear inverse problems. *SIAM Journal on Imaging Sciences*, 2009. 2(1): pp. 183-202. doi: 10.1137/080716542

[11] Daubechies, I., Defrise, M., De Mol, C.. An iterative thresholding algorithm for linear inverse problems with a sparsity constraint. *Communications on pure and applied mathematics*, 2004. 57(11): pp. 1413-1457. doi: 10.1002/cpa.20042

[12] Watermann, J., Bust, G.S., Thayer, J.P., Neubert, T., Coker, C.. Mapping plasma structures in the high-latitude ionosphere using beacon satellite, incoherent scatter radar and ground-based magnetometer observations. *Annals of Geophysics*, 2002. 45(1): pp. 177-189. doi: 10.4401/ag-3488

[13] Fremouw, E.J., Secan, J.A., Howe, B.M.. Application of stochastic inverse theory to ionospheric tomography. *Radio Sci.*, 1992. 27(5): pp. 721-732. doi: 10.1029/92RS00515

[14] Sutton, E., Na, H.. High resolution ionospheric tomography through orthogonal decomposition, in:*IEEE International Conference on Image Processing*. 13-16 Nov 1994. Austin, TX. Los Alamitos: IEEE Computer Society Press. 1994. 148-152. doi: 10.1109/ICIP.1994.413549

[15] Mallat, S.. *A wavelet tour of signal processing: the sparse way*. 3rd ed. Burlington, MA: Academic press. 2008. 832 p.

[16] Hargreaves, J.K., Gadsden, M.. *The Solar-Terrestrial Environment: An Introduction to Geospace - the Science of the Terrestrial Upper Atmosphere, Ionosphere, and Magnetosphere*. New York: Cambridge University Press. 1995. 284 p. doi: 10.1017/CBO9780511628924